Kafkas Universitesi Veteriner Fakultesi Dergisi
ISSN: 1300-6045 e-ISSN: 1309-2251
Journal Home-Page: http://vetdergikafkas.org

Kafkas Univ Vet Fak Derg
27 (1): 73-82, 2021
DOI: 10.9775/kvfd.2020.24776

RESEARCH ARTICLE

Inhibitory Effect and Mechanism of Oyster Enzymatic Hydrolysate on Lung Metastasis in the Subcutaneous Lewis Lung Cancer Model in Mice

Qi-Guan JIN [1,†,a (*)] Ming ZHOU [2,†,b] Yu-Long HU [1,c] Liang CHEN [2,d] Yu LIU [1,e]
Yu-Qing WANG [2,f] Mei-Tong WU [1,g] Rui-Xue ZHANG [2,h] Wen-Ying LIU [2,i (*)]

[†] *These authors have contributed equally to this work*
[1] College of Physical Education, Yangzhou University, Yangzhou 225127, Jiangsu, CHINA
[2] Beijing Engineering Research Center of Protein and Functional Peptides, China National Research Institute of Food and Fermentation Industries Co., Ltd., Beijing 100015, CHINA
ORCIDs: [a] 0000-0002-5539-8779; [b] 0000-0003-4485-9098; [c] 0000-0002-3139-8061; [d] 0000-0002-0692-3960; [e] 0000-0002-6017-5334
[f] 0000-0002-7290-9171; [g] 0000-0002-7404-0158; [h] 0000-0002-1432-2989; [i] 0000-0001-8369-0809

Article ID: KVFD-2020-24776 Received: 27.07.2020 Accepted: 26.11.2020 Published Online: 27.11.2020

Abstract

In order to investigate the inhibitory effects of oyster enzymatic hydrolysate (OEH) on the metastasis of Lewis lung cancer and to evaluate its mechanism, daily gavage of low(LOEH), medium(MOEH) and high (HOEH) doses of OEH for 5 weeks was administered based on the subcutaneous Lewis lung cancer model in C57BL/6J male mice, the volume and weight of subcutaneous tumor were measured, the lung metastatic nodules were counted, the number of tumor-associated-macrophages (TAMs; CD11b+F4/80+), the expression of E-cadherin, Vimentin, microRNA-21 and microRNA-218 in subcutaneous tumor were measured. It was found that OEH treatment significantly decreased the subcutaneous tumor weight for the MOEH and HOEH groups (P=0.013, P=0.007) and significantly inhibited lung metastasis in a dose-dependent manner ($\chi 2$=13.16, P=0.004). The expression of E-cadherin showed a statistical increase at high dose, while the expression of Vimentin and the number of TAMs in subcutaneous tumor was significantly decreased at all OEH doses (P<0.05). The expression of microRNA-21 was significantly decreased in the group of MOEH (P=0.013) and HOEH (P=0.013), and the expression of microRNA-218 was significantly increased in all group with OEH treatment (P<0.05). In conclusion, OEH significantly reduced the growth of subcutaneous tumors and incidence of lung metastases in a dose-dependent manner. Its anti-tumorigenic activity might be explained by its ability to inhibit epithelial mesenchymal transition by reducing the number of TAMs, and down-regulate microRNA-218 as well as up-regulate microRNA-21 expression.

Keywords: *Oyster enzymatic hydrolysate (OEH), Lung metastasis of Lewis lung cancer, Vimentin, Tumor- associated-macrophages (TAMs), microRNA-21, microRNA-218*

Farelerde Subkutan Lewis Akciğer Kanseri Modelinde İstiridye Enzimatik Hidrolizatının Akciğer Metastazı Üzerine Önleyici Etkisi ve Mekanizması

Öz

İstiridye enzimatik hidrolizatının (OEH) Lewis akciğer kanserinin metastazı üzerine inhibitör etkisinin araştırılması ve inhibitör mekanizmanın aydınlatılması amacıyla subkutan Lewis akciğer kanseri modeline göre C57BL / 6J erkek farelerde 5 hafta boyunca OEH'in düşük (LOEH), orta (MOEH) ve yüksek (HOEH) dozlarının günlük gavajı uygulandı. Subkutan tümörün hacmi ve ağırlığı ölçüldü, akciğer metastatik nodüller sayıldı, tümör ilişkili makrofajlar (TAM; CD11b+F4/80+) sayıldı, deri altı tümör yapılarda E-kaderin, Vimentin, microRNA-21 ve microRNA-218 ekspresyonu ölçüldü. OEH'in MOEH ve HOEH sağaltım gruplarının subkutan tümör ağırlığını önemli ölçüde azalttığı (P=0.013, P=0.007) ve doza bağlı olarak akciğer metastazını önemli ölçüde engellediği ($\chi 2$=13.16, P=0.004) saptandı. E-kaderin ekspresyonu, yüksek dozda istatistiksel bir artış gösterirken, tüm OEH gruplarında Vimentin ekspresyonu ve subkutan tümördeki TAM hücre sayısında önemli ölçüde azalma saptandı (P<0.05). MikroRNA-21 ekspresyonu MOEH (P=0.013) ve HOEH (P=0.013) gruplarında önemli ölçüde azalırken ve microRNA-218 ekspresyonunda OEH tedavisi alan tüm gruplarda anlamlı bir artış saptandı (P<0.05). Sonuç olarak, OEH, deri altı tümörlerin gelişimi ve akciğer metastaz insidansını doza bağlı olarak önemli ölçüde azaltmıştır. Anti-tümörojenik aktivitesi, TAM'ların sayısını azaltarak epitelyal mezenkimal geçişi inhibe etme kabiliyeti ve mikroRNA-218'in ekspresyonunu azaltma ve mikroRNA-21'in ekspresyonunu artırma özelliği ile açıklanabilir.

Anahtar sözcükler: *Oİstiridye enzimatik hidrolizatı (OEH), Lewis akciğer kanserinin akciğer metastazı, Vimentin, Tümör ilişkili makrofajlar (TAM), MikroRNA-21, MikroRNA-218*

How to cite this article?

Jin QG, Zhou M, Hu YL, Chen L, Liu Y, Wang YQ, Wu MT, Zhang RX, Liu WY: Inhibitory effect and mechanism of oyster enzymatic hydrolysate on lung metastasis in the subcutaneous lewis lung cancer model in mice. *Kafkas Univ Vet Fak Derg,* 27 (1): 73-82, 2021.
DOI: 10.9775/kvfd.2020.24776

(*) Corresponding Authors

Tel: +86 514 87972015
E-mail: qgjin@yzu.edu.cn (QG Jin); wenyingliu888@126.com (WY Liu)

Introduction

Small cell lung cancer (SCLC) and non-small cell lung cancer (NSCLC) are the main pathological types of lung cancer, for which NSCLC accounts for 85-90% [1]. As the most common cancer in the world, its rates of incidence and mortality are the highest of the malignant tumors, with increasing tendency each year [2]. It is highly invasive, and most patients have metastasis, with 80% of lung cancer patients in the middle and late stage, at the time of diagnosis [3]. Despite the use of surgery, chemotherapy, radiotherapy, molecular targeting and other comprehensive treatments, drug resistance and recurrence are common, and the 5-year survival rate is less than 14% [4].

The recurrence and metastasis of lung cancer have been shown to be closely related to epithelial mesenchymal transition (EMT). EMT can change the phenotype of tumor cells, so that they can obtain stronger invasion and metastasis ability [5]. Down regulation of E-cadherin expression and up regulation of Vimentin expression are important features of EMT [6]. EMT may also be induced by tumor-associated-macrophages (TAMs), which are the most abundant cells in the tumor immune microenvironment and have been shown to reduce the expression of E-cadherin and other epithelial adhesion proteins and increase the expression of Vimentin [7]. Therefore, TAM and EMT play important roles in the occurrence and development of lung cancer.

Studies have suggested that microRNA-218 (miR-218) and microRNA-21 (miR-21) can regulate the proliferation and invasion of tumor cells, thus affecting the prognosis, survival, rate of recurrence and metastasis in lung cancer patients. MiR-218 is down-regulated in NSCLC, which leads to the proliferation of lung cancer cells, increases the probability of recurrence and metastasis, and reduces the survival period for lung cancer patients [8-10]. MiR-21 promotes the invasion and metastasis of NSCLC cells by inhibiting the expression of PTEN and other tumor suppressor genes [11]. Therefore, the down-regulation of miR-218 expression and up-regulation of miR-21 expression are associated with poor prognosis in lung cancer.

Oyster is not only a kind of seafood with tender meat, fresh taste and high nutritional value, but also a common Chinese medicine in the Chinese Pharmacopoeia [12]. Oyster meat is rich in protein, amino acid, taurine, bioactive peptide, fatty acid, glycogen, vitamin and inorganic salt [13], it is often used to enhance immune function, reduce blood glucose and blood lipid and anti-tumor and so on [14-17]. Oyster bioactive peptide, a component of oyster enzymatic hydrolysate (OEH), has been shown to improve cellular immune function and inhibit the growth of malignant tumors [18]; however, it is not clear whether it can inhibit the metastasis of lung cancer, and its mechanism has not been fully elucidated. Mouse model of Lewis lung cancer (LLC) is the most widely used lung cancer model of the same origin, LLC cell line is an adenocarcinoma and maintains high tumorigenicity and lung metastasis in C57BL/6 mice [19,20], and the lung metastasis can be determined after subcutaneous inoculation of LLC cells in C57BL/6 mice for 17-21 days [21]. Therefore, in order to explore the inhibitory effects of OEH on the lung metastasis from subcutaneous tumor cells and to evaluate its mechanism, we established the subcutaneous Lewis lung cancer model in mice [20,21] and treated tumor-bearing mice with OEH at low, medium and high doses. The weights of subcutaneous tumor were measured, lung metastatic nodules were observed and counted, and the percentage of TAMs (CD11b + F4/80+) cells in subcutaneous tumor were detected by flow cytometry. Furthermore, the expression of E-cadherin, Vimentin, miR-21 and miR-218 in subcutaneous tumor was detected by qRT-PCR. Our results provide an experimental basis for the application of OEH in clinical adjuvant treatment of tumors.

Material and Methods

Preparation of OEH

A thousand gram fresh oyster meat *(Crassostrea rivularis)* (Beijing zhongshihaishi biotechnology Co., Ltd) were crashed with a blender, fix the volume to 3 L with distilled water, and put it in boiling water bath for 1 h, then lower it to room temperature, and centrifugated with 3000 g for 5 min. Add 500 mL distilled water to the precipitate and stir well, adjust the pH value to 7.0 with NaOH, put it in the water bath, and raise the temperature to 50°C. Neutral protease (Novozyme Biotechnology Co., Ltd) was added at an amount of 20.000 U per 100 g of raw materials, and after 1 h of enzymolysis, papain (Novozyme Biotechnology Co., Ltd) was added at an amount of 32.000 U per 100 g of raw materials, and the enzymolysis continued for 2 h. The enzyme was then inactivated at 100°C for 15 min. After cooling, centrifugated 3000 g for 10 min and the supernatant was taken to filter by 100 mesh sieve and dry by spray dryer, and dried powder of oyster hydrolysate was obtained.

Animal

Forty-eight SPF-grade 6-week-old male C57BL/6J mice, weighing 20±2 g, were purchased from the comparative medical center of Yangzhou University, they were housed under a natural photoperiod (12 hlight:12 h dark) with suitable temperature (20-25°C), and *ad libitum* food and drinking water. All the experiments that involve animals were approved by the Experimental Animal Management Committee and Experimental Animal Ethics Committee of Yangzhou University (Yzu DWLL-201804-003) and was conducted in compliance with the principles stated in the Guide for the Care and Use of Laboratory Animals (NIH) [22].

Establishment of the Lewis Lung Cancer Mouse Model

The LL/2 mouse Lewis lung cancer cell line (American strain Preservation Center; provided by Shanghai Jining Industrial Co., Ltd) was cultured incomplete Dulbecco Modified Eagle Medium (DMEM, Sigma-Aldrich) containing

10% fetal bovine serum (FBS, Hyclone) at 37°C in a 5% CO_2 incubator. At confluency, the cells were passaged1:3. Cells in logarithmic growth phase were digested with 0.25% pancreatin (Beyotime Biotechnology Co., Ltd.), centrifuged for 5 min (1000 r/min), and resuspended in normal saline. The percentage of living cells, as determined by Trypan blue (Beyotime Biotechnology Co., Ltd.) staining, was more than 95%. The cell concentration was adjusted to 6×10^6 cell/mL, and then 0.2 mLwas inoculated subcutaneously into the right forelimb armpits of C57BL/6J mice [23]. The entire process was strictly sterile and was completed within 40 min.

Grouping and Administration

After 24 h, the mice were weighed, numbered, and randomly divided into the control group (C), low dose OEH intervention group (LOEH), medium dose OEH intervention group (MOEH), and high dose OEH intervention group (HOEH) (12 mice per group). In group C, 0.9% normal saline was given every day after lung cancer cells were inoculated. For the LOEH, MOEH and HOEH groups, OEH was intragastric administered at doses of 0.8 g/kg, 1.8 g/kg and 2.5 g/kg per day for 5 weeks [24].

Sample Collection

The mice were sacrificed after anesthesia, which was performed with 1% pentobarbital sodium according to the body weight (0.05 mL/10 g). The whole subcutaneous tumor was quickly removed, weighed, and divided into three parts. One part was quickly submerged into 10% formaldehyde solution for fixation to diagnose subcutaneous tumor by observing its histological structure; one part was put into a cryopreservation tube, quickly submerged into liquid nitrogen, and stored at −80°C for testing, the other part was processed as a tumor cell suspension for testing the corresponding index. Then, the whole lung tissue was taken and placed in Bouin fixative solution to observe the lung metastasis from subcutaneous tumor by counting the pulmonary surface nodules [25] and Hematoxylin-eosin (HE) staining [26].

Determination of Indicators

Determination of OEH composition: The contents of total protein, acid soluble protein and total sugar in OEH were determined by Kjeldahl method(QSY-IIKjeldahl nitrogen determinator, Beijing Qiangsheng analytical instrument manufacturing center), three chloroacetic acid method and the reagent method (22100 UV spectrophotometer, Unocal Shanghai Instruments Co., Ltd), the composition and content of free amino acids were determined by amino acid automatic analysis(835-50 amino acid analyzer, Hitachi Limited), ash and water were determined by burning method and atmospheric drying method, and the distribution range of molecular weight was determined by high performance liquid chromatography (HPLC)(LC-20a high performance liquid chromatograph, Shimadzu, Kyoto, Japan) [27].

Identification of peptides from OEH: Nexera X2 Ultra high performance liquid chromatography and triple quadrupole mass spectrometer system (Shimadzu, Kyoto, Japan) were used to identify the peptides from OEH. The mass spectrometry conditions are as follows. Ionization mode: ESI, positive ion mode; ion spray voltage: +4.5 KV; atomization gas flow rate: 3.0 L/min of nitrogen; heating gas flow rate: 10 L/min of nitrogen; dry gas flow rate: 10 L/min of nitrogen; DL temperature: 250°C; heating module temperature: 400°C; ion source temperature: 300°C; scanning mode: multi reaction monitoring (MRM); residence time: 100 ms; delay time: 3 ms [28].

Calculation of the survival rate: The survival and death of mice were recorded every day. After 5 weeks, the survival rate of mice in each group was calculated by the formula: survival rate (%) = (survival number of mice in each group/total number of mice in each group) × 100% [29].

Calculation of the tumor inhibition rate: After the establishment of the subcutaneous Lewis lung cancer model, subcutaneous tumor formation was observed each week. The length diameter (L) and width diameter (W) of the tumor were measured with a Vernier ruler, and the tumor volume was calculated with the formula, $V = 1/2 \times L \times W^2$. The average tumor weights for each group were measured and used to calculate the tumor inhibition rate as follows: the tumor inhibition rate (%) = (1 − average tumor weight of experimental group/average tumor weight of control group) × 100% [25].

Calculation of the number of pulmonary surface nodules and the rate of metastasis inhibition: After the lung tissue was fixed in Bouin fixative solution for 24 h, it was soaked in absolute ethanol for 24 h, and the number of pulmonary metastases (visualized as white nodules) was recorded [25].

The lung metastasis rate was calculated as follows: lung metastasis rate = (number of lung metastasis/number of samples in each group) × 100%. The inhibition rate of lung metastasis was calculated as follows: Lung metastasis inhibition rate (%) = (mean number of pulmonary surface metastasis nodules in the model group - mean number of pulmonary surface metastasis nodules in the treatment group)/mean number of pulmonary surface metastasis nodules in the model group × 100% [25].

HE staining: For histological analysis, the subcutaneous tumor and lung tissues were embedded in paraffin, sliced at a thickness of 5 μm and stained with HE. Then histological structure of subcutaneous tumor and lung metastases were observed under light microscope (Olympus, Japan). The histopathological scores were graded according to the severity of the tumor cells affected lung tissue in each HE-stained section, as follows: 1 = minimal (<1%); 2 = slight (1-25%); 3 = moderate (26-50%); 4 = moderate/severe (51-75%); and 5 = severe/high (76-100%) [30,31].

Detection of E-cadherin and Vimentin mRNA expression in

subcutaneous tumor: The mRNA expression of E-cadherin and Vimentin in subcutaneous tumor was detected by qRT-PCR. RNA was isolated from 100 mg subcutaneous tumor tissues with 2 mL RNAiso Plus (Takara Biotechnology Co., Ltd). After extracting the total RNA, a NanoDrop ND-3300 micro spectrophotometer was used to detect the 260/280 absorbance ratio as a measure of RNA purity. The genomic DNA was removed according to the instructions of the cDNA synthesis kit (Takara Biotechnology), and then cDNA was synthesized using a 2720 thermal cycler (USA). The cDNA was stored at −20°C. Amplification was performed on the ABI 7500 thermocycler with the following procedure: pretreatment at 50°C for 2 min, pre-denaturation at 95°C for 10 min, denaturation at 95°C for 15 s, and annealing at 60°C for 60 s, with 40 cycles in total. At the end of the program, the CT value of the target gene and the internal reference (GAPDH) were standardized to calculate the relative expression of the target gene. The SYBR prime script TM RT Master Mix Kit was purchased from Novozin Biotechnology Co., Ltd. Primers for E-cadherin, Vimentin and GAPDH were designed and synthesized by Shanghai Bioengineering Co., Ltd. The primer sequences are shown in *Table 1*.

Detection of TAM (CD11b+F4/80+) cells in subcutaneous tumor: F4/80/CD11b antibody (BD Company) was added to 100 μL of cell suspension, which was incubated in the dark for 20 min. The cells were centrifuged at 300 g for 5 min and resuspended in 100 μL PBS, and then 0.5 μL DAPI was added. The cells were then incubated for 15 min, and 300 μL PBS was added. The amount of TAMs (CD11b+F4/80+) in lung cancer tissue was detected by Cyto FLEX flow cytometry.

Detection of miR-21 and miR-218 expression in subcutaneous tumor: miRNA was isolated using the rapid tissue Cell miRNA extraction kit, and then cDNA was synthesized using the HG TaqMan miRNA reverse transcription kit. Gene amplification was performed on the ABI 7500 with the following program: 15 min at 95°C, 10 s at 95°C and 60 s at 60°C, with 40 cycles. The CT value of the target gene was standardized to the internal reference (RNU6B), and the relative expression was calculated bythe$2^{-\Delta\Delta CT}$ method. The rapid tissue Cell miRNA extraction kit, HG TaqMan miRNA reverse transcription kit, and HGSYBR Green quantitative PCR kit were provided by Haiji Biotechnology Co., Ltd.

Statistical Analysis

SPSS 20.0 statistical software was used to process the data. The results are expressed as mean ± SD. One-way ANOVA and multiple comparison or Chi-square test were used for C, LOEH, MOEH and HOEH groups, with $P<0.05$ indicating significant difference.

Results

Composition of OEH

As shown in *Table 2*, the total protein content of OEH is 57.23%, acid soluble protein content is 52.12%, and acid soluble protein accounts for 91.07% of the total protein content. The total sugar content was 25.89%, and the free amino acid content was 6.16%. Because small peptide and free amino acids can be dissolved in acid solution [19], the content of small molecule oligopeptides in OEH is about 45.96%. The relative molecular weight was less than 1000 Da in OEH was 91.92%, indicating that the main components of OEH not only contain small molecular oligopeptides, but also rich in oyster polysaccharides and other substances.

The Sequences of Peptides in OEH

To identify the peptide sequences, OEH was subjected to chromatography and mass spectrometer system. OEH is composed of a large number of short peptides, and HPLC-MS/MS spectra processing identified 20 major peptide sequences. *Fig. 1* indicates several peptides with an arginine residue at the C-terminusor N-terminus, whose sequences include Ile-Arg, Arg-Ile and Val-Arg. The molecular mass of Ile-Arg, Arg-Ile and Val-Arg are 287.4, 287.4 and 273.3Da, respectively.

OEH Mediates Dose-Dependent Inhibition of Subcutaneous Tumor Growth in the Lewis Lung Cancer Model in Mice

To evaluate the ability of OEH to inhibit subcutaneous tumor growth in the Lewis lung cancer mouse model, we measured the tumor volume and weight and observed their histological structure in each group of mice. Though there was a trend of volume reduction with increasing OEH, the decrease was not statistically significant ($F=1.168$, $P=0.348$); however, OEH had a significant effect on the weight of subcutaneous tumors in tumor-bearing mice ($F=3.635$, $P=0.032$) *(Table 3)*. The reduction was most obvious at the HOEH dose ($P=0.007$; 36% inhibition rate), with progressively less reduction at the MOEH dose ($P=0.013$;

Table 1. *Sequence of RT-PCR specific primers*

Oligo Name	Orientation	Sequence (5'to3')	%GC	TM
E-cadherin	Forward	TATGATGAAGAAGGAGGTGGAGA	43.48	54.37
	Reverse	AACACCAACAGAGAGTCGTAAGG	47.83	56.56
Vimentin	Forward	AGTATGAAAGCGTGGCTGCC	55	58.50
	Reverse	AGCTTCCTGTAGGTGGCGAT	55	58.50
GAPDH	Forward	GGTTGTCTCCTGCGACTTCA	60	62.62
	Reverse	TGGTCCAGGGTTTCTTACTCC	50	60.47

RT-PCR: *Real time quantitative PCR;* ***GC:*** *Guanine (G) and cytosine (C) content;* ***TM:*** *Melting Temperature;* ***GADPH:*** *Glycerol 3 phosphate dehydrogenase*

Table 2. *Basic composition and molecular weight distribution of OEH*

Basic Composition		Molecular Weight Distribution	
Composition	**Proportion (%)**	**Molecular Weight (Da)**	**Proportion (%)**
Total protein	57.23	5000-10000	0.4477
Acid soluble protein	52.12	3000-5000	0.8412
Free amino acids	6.16	2000-3000	1.2510
Total sugar	25.89	1000-2000	5.4109
Ash	10.46	150-1000	65.8831
Water	6.28	1-150	26.0374

29% inhibition rate) and the LOEH dose (P=0.082; 22% inhibition rate). Consistently, the tumors in the MOEH and HOEH groups were visibly smaller than those in the C and LOEH groups *(Fig. 2-A)*. We also assessed the 5-week survival rate but observed no detectable effect (χ^2 = 2.254, P=0.521). As shown in *Fig. 2-B*, the tumor cell density in group C was high, the outline was clear, the nucleus was large and deep staining, the nucleoplasm ratio was imbalanced, and the nuclear heteromorphism was obvious, with dual or multinucleus visible. The morphology of tumor tissues in the LOEH, MOEH, and HOEH groups changed significantly, the density of tumor cells was reduced, the proportion of deep stained nuclei was relatively reduced, and the nuclei appeared shrinkage or fragmentation. Spotty or patchy necrosis was appeared in tumor tissues, especially in MOEH and HOEH groups. These results suggest that OEH mediates dose-dependent inhibition of subcutaneous tumor growth by promoting the death of tumor cell.

OEH Treatment Decreases the Rate and Histopathological Scores of Lung Metastasis in the Lewis Lung Cancer Model in Mice

To further evaluate the effect of OEH in the Lewis lung tumor model, we assessed pulmonary surface nodule formation as a measure of metastasis. As shown in *Table 4*, OEH had a significant inhibitory effect on the lung metastasis in tumor bearing mice (χ^2=13.16, P=0.004; F=8.795, P=0.001). The rate and histopathological scores of lung metastasis gradually decreased with increasing OEH dose, which suggests dose dependence. The number of nodules also decreased gradually with increasing OEH dose, but the differences were not statistical (F=1.147, P=0.356; *Fig. 3-A)*. However, HE staining of lung sections showed that the lesion scores in group MOEH or HOEH had significantly fewer than that in group C (P=0.001, P=0.000) *(Fig. 3-B)*. Collectively, these results suggest that OEH may decrease lung metastasis or/ and reduce the growth of lung metastases.

OEH Can Modulate the mRNA Expression of Vimentin and E-cadherin in Subcutaneous Tumor

We further assessed the effects of OEH on the expression of Vimentin and E-cadherin as indicators of EMT. As shown in

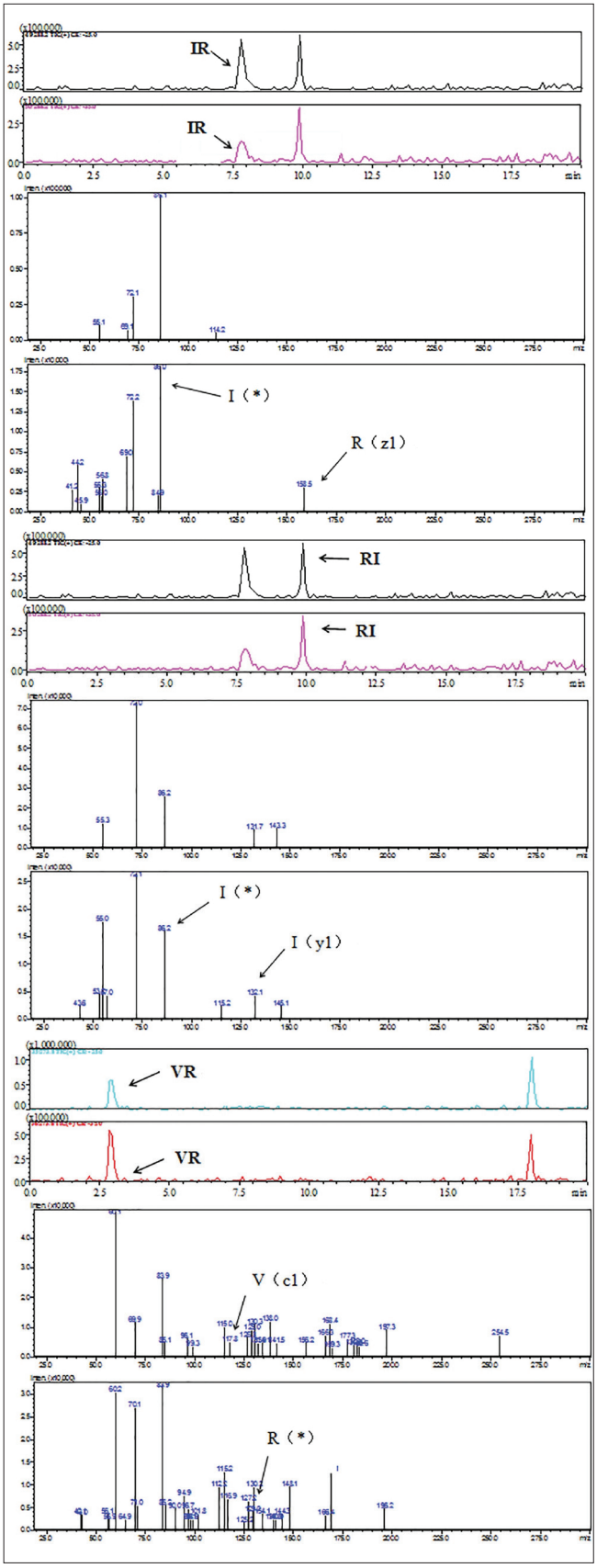

Fig 1. The map of sequence Ile-Arg, Arg-Ile and Val-Arg. HPLC-MS/MS analysis to reveal the structure of peptides with an arginine residue at the C-terminus or N-terminus, whose sequences

Table 3. *Changes in the volume, weight of subcutaneous tumor and tumor inhibition rate in OEH-treated mice (M ± SD)*

Group	n	Volume (mm^3)	Weight (g)	Tumor Inhibition Rate (%)	5-week Survival Rate (%)
C	5	5131.80±2979.03	11.12±1.19	-	42
LOEH	5	4180.90±1018.11	8.70±1.63	22	42
MOEH	8	3821.31±1325.35	7.88±2.42*	29	67
HOEH	5	3074.50±1434.92	7.10±2.50**	36	42

*One-way ANOVA and multiple comparisons or Chi-square test were carried out for groups C, LOEH, MOEH and HOEH, compared with group C. * P<0.05, ** P<0.01. C: control; OEH: oyster enzymatic hydrolysate; LOEH: low doses of OEH; MOEH: medium doses of OEH; HOEH: high doses of OEH*

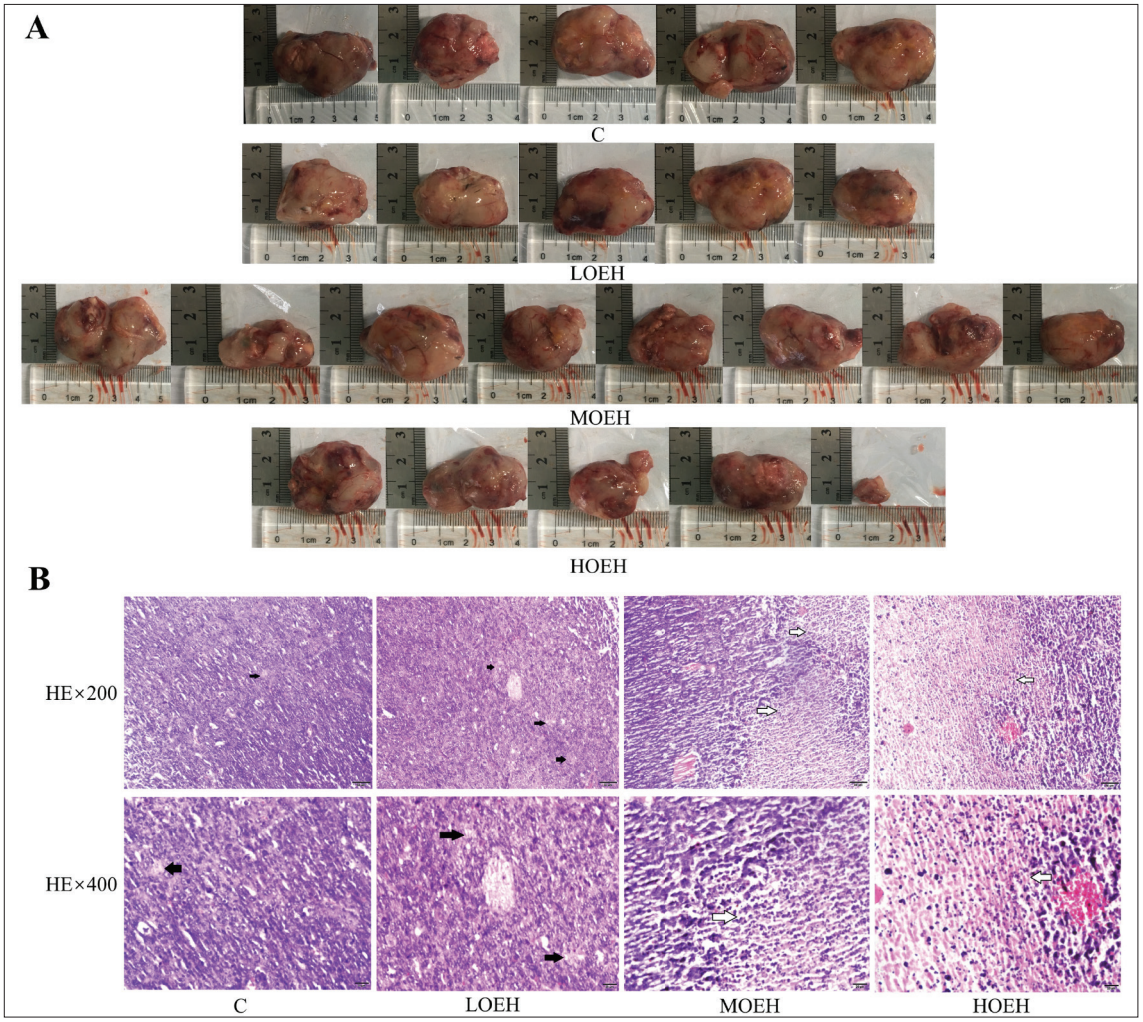

Fig 2. Subcutaneous tumors (A) and their histological structure (B, HE staining, ×200 and ×400) from each group. ↗: Spotty necrosis; ⇨:Patchy necrosis. C: control; OEH: oyster enzymatic hydrolysate; LOEH: low doses of OEH; MOEH: medium doses of OEH; HOEH: high doses of OEH

Table 5, OEH mediated a statistical increase in the expression of E-cadherin mRNA in subcutaneous tumor (F=3.318, P=0.042) and a statistical decrease in the expression of Vimentin mRNA (F=5.609, P=0.006). Compared with group C, the expression of Vimentin mRNA was decreased significantly in the LOEH, MOEH and HOEH groups (P=0.001, P=0.010, P=0.007), however the expression of E-cadherin mRNA was significantly increased only in HOEH group (P=0.014). These results suggest that OEH causes a decrease in Vimentin expression and increase in E-cadherin expression, which might suggest that OEH inhibits EMT.

OEH Treatment Reduce the Counts of TAMs (CD11b + F4/80 + cells) in Subcutaneous Tumor

To further evaluate a potential role for EMT mediating OEH-dependent decrease in tumor growth and metastasis, we assessed the effect of OEH treatment on CD11b + F4/80 + TAMS *(Fig. 4-A)*. As shown in *Fig. 4-B*, OEH mediated an overall significant decrease in the number of CD11b + F4/80 + cells in subcutaneous tumor (F=3.144, P=0.049). Nevertheless, the number of CD11b + F4/80 + cells in the LOEH, MOEH and HOEH group were decreased significantly (P=0.014; P=0.015;

Table 4. *Changes in the lung metastasis inhibition rate, the number of pulmonary surface nodules, and the 5-week survival rate in OEH-treated mice (M ± SD)*

Group	n	Lung Metastasis Rate (%)	Number of Nodules	Lung Metastasis Inhibition Rate (%)	Histopathological Scores
C	5	100.00	3.60±3.21	-	3.20±0.45
LOEH	5	100.00	3.20±1.64	11	2.40±0.55
MOEH	8	87.50	2.25±1.49	36	1.75±0.71**
HOEH	5	20.00**	1.20±2.68	67	1.20±0.84**

*Chi-square test or One-way ANOVA and multiple comparisons were carried out for groups C, LOEH, MOEH and HOEH, compared with group C. ** P<0.01. C: control; OEH: oyster enzymatic hydrolysate; LOEH: low doses of OEH; MOEH: medium doses of OEH; HOEH: high doses of OEH*

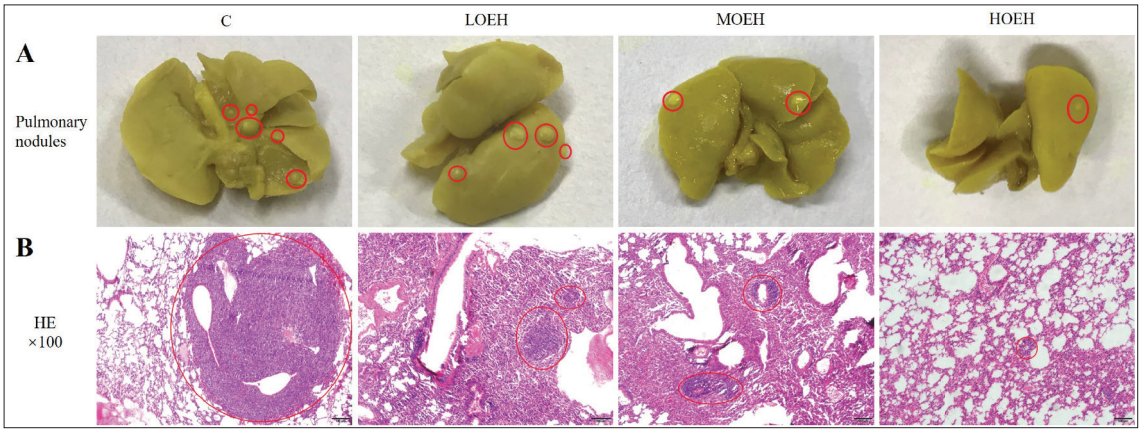

Fig 3. The pulmonary surface nodules (A) and their histological structure (B, HE staining, x100) in each group. The gray and white nodules in the red circle are metastatic tumor. C: control; OEH: oyster enzymatic hydrolysate; LOEH: low doses of OEH; MOEH: medium doses of OEH; HOEH: high doses of OEH

Table 5. *Expression of E-cadherin and Vimentin mRNA in subcutaneous tumor of mice (M ± SD)*

Group	n	E-cadherin	Vimentin
C	5	0.90±0.36	1.09±0.44
LOEH	5	1.08±0.44	0.22±0.06**
MOEH	8	0.96±0.64	0.52±0.44*
HOEH	5	1.74±0.28*	0.42±0.22**

*One-way ANOVA and multiple comparisons were carried out for groups C, LOEH, MOEH and HOEH, compared with group C. * P<0.05, ** P < 0.01. C: control; OEH: oyster enzymatic hydrolysate; LOEH: low doses of OEH; MOEH: medium doses of OEH; HOEH: high doses of OEH*

Table 6. *Expression of miR-21 and miR-218 in subcutaneous tumor of mice (M ± SD)*

Group	n	miR-21	miR-218
C	5	0.96±0.36	1.05±0.16
LOEH	5	0.64±0.25	2.52±0.89*
MOEH	8	0.49±0.28*	2.84±1.04**
HOEH	5	0.43±0.34*	2.83±1.47*

*One-way ANOVA and multiple comparisons were carried out for groups C, LOEH, MOEH and HOEH, compared with group C. * P<0.05, ** P<0.01. C: control; OEH: oyster enzymatic hydrolysate; LOEH: low doses of OEH; MOEH: medium doses of OEH; HOEH: high doses of OEH*

P=0.045) than that in the C group of mice. Therefore, OEH treatment with all dose can decreases the percentage of TAMs (CD11b + F4/80 + cells) in subcutaneous tumor.

Expression of miR-21 and miR-218 is Modulated in Subcutaneous Tumor of Mice with OEH Treatments

To evaluate the potential roles of miR-21 and miR-218 as mediators of OEH-dependent tumor reduction, we measured their expression in group C and each of the treatment groups. OEH had an overall significant effect on the expression of miR-21 and miR-218 in subcutaneous tumor of tumor bearing mice as determined one-way ANOVA (F=3.251, P=0.045; F=3.743, P=0.029). Furthermore, after multiple comparison, the expression of miR-21 significantly decreased in the group of MOEH (P=0.013) and HOEH (P=0.013) *(Table 6)*. And the expression of miR-218 was significantly increased in the group of LOEH (P=0.034), MOEH (P=0.006) and HOEH (P=0.012). These results are consistent with a potential role for miR-21 and miR-218 in mediating the tumor-protective effects of OEH.

Discussion

Oyster enzymatic hydrolysate (OEH) is obtained by enzymolysis, concentration, and freeze-drying of oyster meat. In this study, we found that the content of total protein, total sugar and small molecule oligopeptides in OEH were 57.23%, 25.89% and 45.96%, the relative molecular weightless than 1000 Da was 91.92% in OEH, indicating that the main components of OEH contain not only small molecular oligopeptides, but also rich in oyster polysaccharides. It has been proved that oligopeptides with molecular weight less than 1000 Da are mostly dipeptides and tripeptides [27],

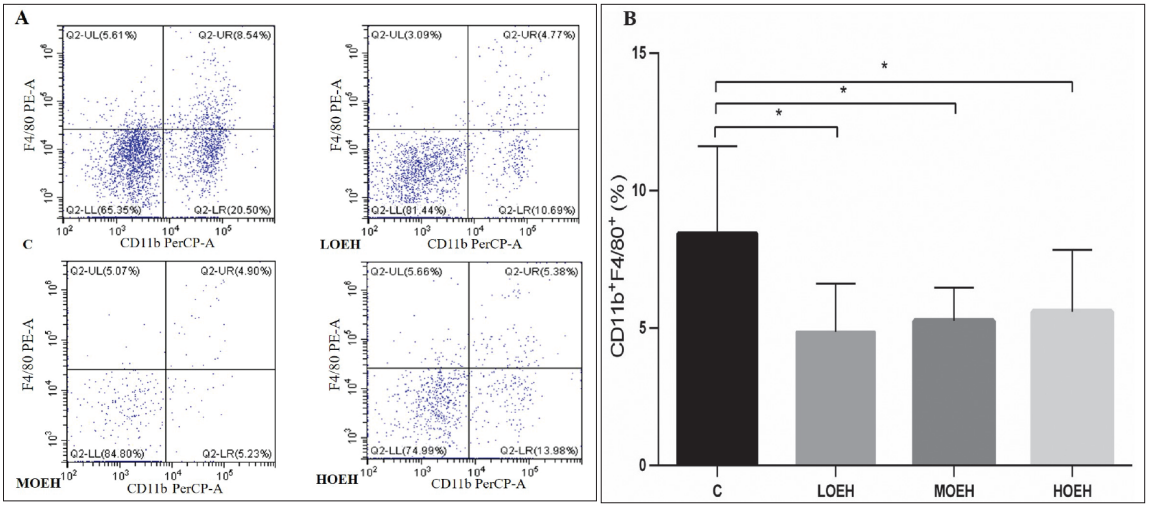

Fig 4. Distribution map (A) and percentage of CD11b+F4/80+ cells in subcutaneous tumor of mice in each group (B). The cells in UR region are CD11b + F4/80 + cells. One-way ANOVA and multiple comparisons were carried out for groups C, LOEH, MOEH and HOEH, compared with group C. * P<0.05. C: control; OEH: oyster enzymatic hydrolysate; LOEH: low doses of OEH; MOEH: medium doses of OEH; HOEH: high doses of OEH

which have faster absorption rate compared with proteins and free amino acids [12,32,33], and oyster polysaccharides can be absorbed without digestion [16]. Therefore, it can be inferred that OEH has not only higher biological activity, but also higher absorption rates than Natural Oyster Protein. At the same time, dipeptides containing arginine were isolated from OEH, and L-arginine supplementation can enhance the immune function of tumor patients, reduce the synthesis of tumor protein, and inhibit the growth of tumor [34,35]. Although the bioactive peptide of oyster has many physiological functions, there are few studies on its antitumor effect. The natural low molecular polypeptide BPO-L, which is extracted from the oyster, has been shown to effectively inhibit the proliferation [36], and change the malignant morphology and ultrastructural characteristics [37] of human lung adenocarcinoma A549 cells.

In this study, we found that increasing OEH doses show a trend of reduction in volume and weight of subcutaneous tumor in tumor-bearing mice, though the changes in tumor volume were not statistically significant, and only the tumor weight reductions in the MOEH (29% decrease) and HOEH (36% decrease) groups were statistically significant. In the meantime, HE staining of tumor tissues showed that the density of tumor cells, nuclear heteromorphism reduced and necrosis area of tumor cells increased gradually with the increase of OEH doses. Because the growth of tumor is related to the proliferation, apoptosis and necrosis of tumor cells, the supplement of OEH can promote the necrosis of tumor cells to inhibit the growth of subcutaneous tumors. Our previous studies confirmed that OEH treatment can effectively improve the function of T cells and NK cells, and increase the apoptosis and necrosis of Lewis lung cancer cells implanted subcutaneously, which can effectively inhibit the growth of subcutaneous implanted tumor [38]. However, whether OEH can inhibit the proliferation of tumor cells remains to be further studied. Furthermore, the lung metastasis rate was decreased significantly with increasing OEH dose. Although the number of lung metastasis nodules had not statistically decrease. HE staining of lung sections showed that the lesion scores in group MOEH or HOEH had significantly fewer than that in group C. Therefore, OEH can inhibit lung metastasis from subcutaneous tumor cells to a certain extent, and/or reduce the growth of lung metastases. However we found that OEH treatment cannot effectively improve the 5-week survival rate of tumor bearing mice, its reason is unclear, which needs further study.

The invasion and metastasis of lung cancer mainly involve a series of rather complex processes, such as cell adhesion, matrix degradation and cell movement [39]. Among them, EMT can change the phenotype of tumor cells, so that they have a strong ability of invasion and metastasis [40]. On the one hand, E-cadherin is an adhesion factor that can inhibit the invasion and metastasis of tumor cells. Decreased E-cadherin expression results in a decrease in the adhesion between homologous cells [41]. On the other hand, Vimentin is a marker of stromal cells and can maintain and promote stromal transformation and invasion of tumor cells. Increased expression of Vimentin marks the occurrence of the EMT process [42]. Therefore, the expression of E-cadherin and Vimentin provides an important reference value for the evaluation of tumor malignancy, invasion depth, prediction of metastasis and prognosis [43]. Studies have also shown that TAMs can promote the growth and metastasis of lung cancer cells, whereas inhibition of the aggregation of TAMs in tumors can improve the prognosis of lung cancer [44-48]. In this study, we observed that OEH supplementation with all dose could significantly reduce TAMs and Vimentin mRNA expression in subcutaneous tumor, though only increase of E-cadherin mRNA expression at high dose was statistically significant. Therefore, it is possible that the inhibition of tumor growth and invasion by OEH is mediated by inhibition of EMT.

MicroRNAs are a group of noncoding RNAs that regulate gene transcription and protein translation at the post transcriptional level and play important roles in cell proliferation, differentiation and apoptosis [49,50]. The expression of miR-218 has been shown to be down-regulated or absent in lung cancer cells [51,52]. MiR-218 inhibits the invasion and migration of lung cancer cells by inhibiting the expression of Robo1 and can promote apoptosis of A549 cells by negatively regulating the expression of its target gene, SFMBT1 [53]. On the other hand, the high expression of miR-21 in NSCLC is closely related to NSCLC cell proliferation, angiogenesis, invasion and metastasis [54,55], as well as poor prognosis in NSCLC [56], for which it serves as a potential molecular target for lung cancer diagnosis, metastasis and prognosis. Inhibition of miR-21 can induce apoptosis and inhibit proliferation of cancer cells and can enhance the sensitivity of cancer cells to chemotherapy drugs and radiotherapy [57,58]. Consequently, miR-21 plays an oncogenic role while miR-218 plays a tumor suppressor role. In this study, oral OEH with all dose could significantly up-regulate the expression of miR-218, although only medium and high dose of OEH could significantly down-regulate the expression of miR-21. Therefore, OEH can modulate the expression of miR-21 and miR-218 in subcutaneous tumor to a certain extent, which may explain its ability to inhibit the lung metastasis from subcutaneous tumor cells.

In conclusion, the main components of OEH contain small molecular oligopeptides, oyster polysaccharides and other substances. OEH can significantly reduce the growth of subcutaneous tumor and lung metastasis in a dose-dependent manner. It can also modulate the mRNA expression of Vimentin and E-cadherin in subcutaneous tumor and reduce the number of TAMs at specific doses. OEH increases the expression of miR-21 and inhibits the expression of miR-218 in subcutaneous tumor in a dose-dependent manner, which might explain, in part, its inhibitory effect on the lung metastasis from subcutaneous tumor cells.

Acknowledgements

We are grateful to the guidance and help of Professor Xiao-Qin Jia from Medicine college of Yangzhou University and Dr. Lei Wang from the Affiliated Hospital in the histopathological research of this paper.

Declaration of Conflicting Interests

The authors declare no potential conflicts of interest with respect to the research, authorship, and/or publication of this article.

Funding

This work was supported by National Key Research and Development project in China (Grant No: 2016YFD0400603) and Open Project of the Beijing Engineering Research Center of Protein and Functional Peptides (Grant No: 2017PFP001).

Author Contributions

Q.G. JIN and W.Y. LIU planned and designed the research. Q.G. JIN and W.Y. LIU had a role in manuscript drafting and in process of revision. M. ZHOU, L. Chen, Y.Q. WANG and R.X. ZHANG carried out the preparation and identification of OEH in the study. Y.L. HU, Y. LIU and M.T. WU performed experiments. Y. LIU, Y.L.HU and Q.G. JIN carried out the statistical analysis. All authors have interpreted the data, revised the manuscript, and approved the final version.

References

1. Goldstraw P, Crowley J, Chansky K, Giroux DJ, Groome PA, Rami-Porta R, Postmus PE, Rusch V, Sobin L, International Association for the Study of Lung Cancer International Staging Committee, Participating Institutions: The IASLC lung cancer staging project: Proposals for the revision of the TNM stage groupings in the forthcoming (seventh) edition of the TNM classification of malignant tumours. *J Thorac Oncol*, 2 (8): 706-714, 2007. DOI: 10.1097/JTO.0b013e31812f3c1a

2. Torre LA, Bray F, Siegel RL, Ferlay J, Lortet-Tieulent J, Jemal A: Global cancer statistics, 2012. *CA Cancer J Clin*, 65 (2): 87-108, 2015. DOI: 10.3322/caac.21262

3. Nie LG: Screening for lung cancer-Opportunities and challenges. *Chin J Lung Cancer*, 18 (12): 721-724, 2015. DOI: 10.3779/j.issn.1009-3419.2015.12.01

4. Herbst RS, Morgensztern D, Boshoff C: The biology and management of non-small cell lung cancer. *Nature*, 553, 446-454, 2018. DOI: 10.1038/nature25183

5. Gu K, Li MM, Shen J, Liu F, Cao JY, Jin S, Yu Y: Interleukin-17-induced EMT promotes lung cancer cell migration and invasion via NF-κB/ZEB1 signal pathway. *Am J Cancer Res*, 5 (3): 1169-1179, 2015.

6. Lamouille S, Xu J, Derynck R: Molecular mechanisms of epithelial-mesenchymal transition. *Nat Rev Mol Cell Biol*, 15, 178-196, 2014. DOI: 10.1038/nrm3758

7. Galdiero MR, Garlanda C, Jaillon S, Marone G, Mantovani A: Tumor associated macrophages and neutrophils in tumor progression. *J Cell Physiol*, 228 (7): 1404-1412, 2013. DOI: 10.1002/jcp.24260

8. Chen J: Expression of miRNA-218 in non-small cell lung cancer and its relationship with prognosis. *J Clin Pulm Med*, 24 (6): 1102-1104, 2019. DOI: 10.3969/j.issn.1009-6663.2019.06.035

9. Luan L, Han B, Wang CF, Bai Y, Teng M, Huan DW, Xu HT, Wang EH: MiR-218-1-3p expression in non-small cell lung cancer and its clinical significance. *J China Med Univ*, 43 (2): 181-183, 2014.

10. Zhang CL, Ge SL, Hu CL, Yang N, Zhang JR: MiRNA-218, a new regulator of HMGB1, suppresses cell migration and invasion in non-small cell lung cancer. *Acta Biochim Biophys Sin*, 45 (12): 1055-1061, 2013. DOI: 10.1093/abbs/gmt109

11. Liu ZL, Wang H, Liu J, Wang ZX: MicroRNA-21 (miR-21) expression promotes growth, metastasis, and chemo-or radioresistance in non-small cell lung cancer cells by targeting PTEN. *Mol Cell Biochem*, 372, 35-45, 2013. DOI: 10.1007/s11010-012-1443-3

12. Fang L, Ma HX, Li LH, Yang XQ, Rong H, Zhu CB: Analysis and evaluation of nutrient composition in Ostrea rivularis from south China sea coast. *Sci Tech Food Indus*, 39 (2): 301-307, 2018. DOI: 10.13386/j.issn1002-0306.2018.02.056

13. Fang L, Li GM, Xu SS, Lu L, Gu RZ, Cai MY, Lu J: Research progress of bioactive peptides from oyster. *J Food Saf Qual*, 9 (7): 1548-1553, 2018. DOI: 10.3969/j.issn.2095-0381.2018.07.015

14. Dai CM, Liao XY, Ye ZG: Review on chemical composition, pharmacological activity and application of Marine Traditional Chinese Medicine Oyster. *Nat Prod Res Dev*, 28(3): 471-474, 2016. DOI: 10.16333/j.1001-6880.2016.3.028

15. Feng L, Zhao WJ, Chang WZ: Research progress in the pharmacological action and clinical application of oyster. *Inf Tradit Chin Med*, 28 (1): 114-116, 2011.

16. Li CZ, Pan ZF, Chen YH, Zhang YQ, Huang XR, Huang JX: Research progress in active substance of oyster softbody. *Sci Tech Food Indus*, 33 (8): 412-415, 2012. DOI: 10.13386/j.issn1002-0306.2012.08.105

17. Zhao XL: Study on the biological activity of oyster and its food development. *Jiangsu Condiment and Subsidiary Food*, 26 (4): 37-41, 2009. DOI: 10.16782/j.cnki.32-1235/ts.2009.04.013

18. Umayaparvathi S, Meenakshi S, Vimalraj V, Arumugam M, Sivagami G, Balasubramanian T: Antioxidant activity and anticancer effect of bioactive peptide from enzymatic hydrolysate of oyster *(Saccostrea cucullata). Biomed Prev Nutr*, 4 (3): 343-353, 2014. DOI: 10.1016/j.bionut.2014.04.006

19. Bertram JS, Janik P: Establishment of a cloned line of Lewis lung carcinoma cells adapted to cell culture. *Cancer Lett*, 11 (1): 63-73, 1980. DOI: 10.1016/0304-3835(80)90130-5

20. Zhu H, Kauffman ME, Trush MA, Jia ZQ, Li YR: A simple bioluminescence imaging method for studying cancer cell growth and metastasis after subcutaneous injection of Lewis lung carcinoma cells in syngeneic C57BL/6 mice. *React Oxyg Species (Apex)*, 5 (14): 118-125, 2018. DOI: 10.20455/ros.2018.813

21. Ma XM, Yu MW, Zhang GL, Yu J, Cao KX, Sun X, Yang GW, Wang XM: Comparison of mouse models of Lewis lung carcinoma subcutaneously transplanted at different sites. *Acta Lab Anim Sci Sin*, 25 (4): 386-390, 2017. DOI: 10.3969/j.issn.1005-4847.2017.04.008

22. National Research Council (US) Committee for the Update of the Guide for the Care and Use of Laboratory Animals: Guide for the Care and Use of Laboratory Animals. 8th ed., *Washington (DC): National Academies Press (US)*, 2011. DOI: 10.17226/12910

23. Zhou LP, Ma K, Ma ZG, Bian J, Zhou H, Ji XE, Li SY: Effect of jian-pi-bu –shen-fang synergism chemotherapy on mice lewis lung cancer cells and its ultrastructure. *J Ningxia Med Univ*, 37 (7): 755-758, 2015. DOI: 10.16050/j.cnki.issn1674-6309.2015.07.008

24. Xu D, Lin F, Zhu XY, Liu WY, Chen XW, Feng JQ, Fan AQ, Cai MY, Xu YJ: Immunomodulatory effect of oyster peptide on immunosuppressed mice. *J Peking Univ (Health Sci)*, 48 (3): 392-397, 2016. DOI: 10.3969 /j.issn.1671-167X.2016.03.003

25. Tang M, Wang SM, Wei YL, Fu JT: Inhibition effects of Yuxiao San combined with cisplatin on transplanted tumor growths via upregulation of nm-23 and downregulation of K-ras in Lewis lung cancer mice. *Oncol Lett*, 17 (1): 1267-1273, 2019. DOI: 10.3892/ol.2018.9673

26. Zhou QQ, Zhang Z, Song LY, Huang CH, Cheng Q, Bi SX, Hu XJ, Yu RM: Cordyceps militaris fraction inhibits the invasion and metastasis of lung cancer cells through the protein kinase B/glycogen synthase kinase 3β/βcatenin signaling pathway. *Oncol Lett*, 16, 6930-6939, 2018. DOI: 10.3892/ol.2018.9518

27. Zhang JT, Qin XY, Jia FH, Yuan Y, Zhou M, Fang L, Zhang RX, Gu RZ, Liu WY: In vitro antioxidation and ACE inhibition of ovalbumin oligopeptides. *Food Ferment Indus*, 45 (12): 67-74, 2019. DOI: 10.13995/j.cnki.11-1802/ts.019561

28. Gu RZ, Liu WY, Lin F, Jin ZT, Chen L, Yi WX, Lu J, Cai MY: Antioxidant and angiotensin I-converting enzyme inhibitory properties of oligopeptides derived from black-bone silky fowl *(Gallus gallus domesticus Brisson)* muscle. *Food Res Int*, 49 (1): 326-333, 2012. DOI: 10.1016/j.foodres.2012.07.009

29. Wang ZF, Yang HY, Liu XB, Zhang RX, Liu SL: Effect of topotecan on survival and tumor metastasis of non-small cell lung cancer mouse models and its mechanism. *Oncol Prog*, 18 (1): 26-29,61, 2020.

30. Hsieh PF, Chueh PJ, Liu PF, Liao JW, Hsieh MK: Immune response evoked by tumor-associated NADH oxidase (tNOX) confers potential inhibitory effect on lung carcinoma in a mouse model. *Am J Cancer Res*, 9 (4): 740-751, 2019.

31. Shackelford C, Long G, Wolf J, Okerberg C, Herbert R: Qualitative and quantitative analysis of nonneoplastic lesions in toxicology studies. *Toxicol Pathol*, 30 (1): 93-96, 2002. DOI: 10.1080/01926230252824761

32. Chen YH, Li CZ, Li DR: The progress on biological activity and separation of the bioactive peptides of oyster protein. *Food Res Dev*, 36 (15): 135-138, 2015. DOI: 10.3969/j.issn.1005-6521.2015.15.033

33. Lundquist P, Artursson P: Oral absorption of peptides and nanoparticles across the human intestine: Opportunities, limitations and studies in human tissues. *Adv Drug Deliv Rev*, 106 (Pt B): 256-276, 2016. DOI: 10.1016/j.addr.2016.07.007

34. Deng WY, Li N, Xia XX, Luo SX, Li SY: Status and progress of immunonutrition in tumour. *J Chin Oncol*, 20 (8): 619-624, 2014. DOI: 10.11735/j.issn.1671-170X.2014.08.B002

35. Szefel J, Danielak A, Kruszewski WJ: Metabolic pathways of L-arginine and therapeutic consequences in tumors. *Adv Med Sci*, 64 (1): 104-110, 2019. DOI: 10.1016/j.advms.2018.08.018

36. Li QF, Huang DC, Shi SL, Liang Y, Li XQ: The regulation effects of bioactive peptides of oyster (BPO-L) on the cell cycle and gene expression of human lung adenocarcinoma A549 cells. *J Xiamen Univ Nat Sci*, 47 (1): 104–110, 2008. DOI: 10.3321/j.issn:0438-0479.2008.01.023

37. Liang Y, Huang DC, Shi SL, Li QF: Effects of oyster low molecular mass bioactive peptides on the morphology and ultrastucture of human lung adenocarcinoma A549 cells. *J Xiamen Univ Nat Sci*, 45 (z1): 177–180, 2006. DOI:10.3321/j.issn:0438-0479.2006.z1.044

38. Wu MT, Zhang HX, Zhang M, Bi Y, Xu HR, Ling K, Jin QG, Liu WY: Inhibition and mechanism of oyster enzymatic hydrolysate on Lewis lung cancer. *Food Ferment Indus*, 46 (11): 98-104, 111, 2020. DOI: 10.13995/j.cnki.11-1802/ts.023063

39. Ma XP, Zhang H, Wang YP, Zhang L, MaJ, Peng T, Leng J: Down-regulation of E-cadherin upregulates the phosphorylation level of GSK-3β in human hepatoma cells. *Acta Univ Med Nanjing*, 32 (7): 896-902, 2012.

40. Thiery JP, Acloque H, Huang RYJ, Nieto MA: Epithelial-mesenchymal transitions in development and disease. *Cell*, 139, 871-890, 2009. DOI: 10.1016/j.cell.2009.11.007

41. Ko H, So Y, Jeon H, Jeong MH, Choi HK, Ryu SH, Lee SW, Yoon HG, Choi KC: TGF-β1-induced epithelial–mesenchymal transition and acetylation of Smad2 and Smad3 are negatively regulated by EGCG in human A549 lung cancer cells. *Cancer Lett*, 335 (1): 205-213, 2013. DOI: 10.1016/j.canlet.2013.02.018

42. Zhu QS, Rosenblatt K, Huang KL, Lahat G, Brobey R, Bolshakov S, Nguyen T, Ding Z, Belousov R, Bill K, Luo X, Lazar A, Dicker A, Mills GB, Hung MC, Lev D: Vimentin is a novel AKT1 target mediating motility and invasion. *Oncogene*, 30, 457-470, 2011. DOI: 10.1038/onc.2010.421

43. Xia D, Li YM, Tan XN, Kuang C, Guo JS: Effects of Feifukang on the growth of tumor and expression of E-cadherin,vimentin, and TGF-β in mice with Lewis lung cancer. *J Tradit Chin Med Univ Hunan*, 35 (3): 30-33, 2015. DOI: 10.3969/j.issn.1674-070X.2015.03.009.030.04

44. Chanmee T, Ontong P, Konno K, Itano N: Tumor-associated macrophages as major players in the tumor microenvironment. *Cancers*, 6 (3): 1670-1690, 2014. DOI: 10.3390/cancers6031670

45. Mantovani A, Allavena P: The interaction of anticancer therapies with tumor-associated macrophages. *J Exp Med*, 212 (4): 435-445, 2015. DOI: 10.1084/jem.20150295

46. Munn DH, Bronte V: Immune suppressive mechanisms in the tumor microenvironment. *Curr Opin Immunol*, 39, 1-6, 2016. DOI: 10.1016/j.coi.2015.10.009

47. Noy R, Pollard JW: Tumor-associated macrophages: From mechanisms to therapy. *Immunity*, 41 (1): 49-61, 2014. DOI: 10.1016/j.immuni.2014.06.010

48. Ostuni R, Kratochvill F, Murray PJ, Natoli G: Macrophages and cancer: From mechanisms to therapeutic implications. *Trends Immunol*, 36 (4): 229-239, 2015. DOI: 10.1016/j.it.2015.02.004

49. Davalos V, Esteller M: MicroRNAs and cancer epigenetics: A macrorevolution. *Curr Opin Oncol*, 22 (1): 35-45, 2010. DOI: 10.1097/CCO.0b013e328333dcbb

50. Kiran C, Deepika P: Lung cancer: microRNA and target database. *Chin J Lung Cancer*, 15 (7): 429-434, 2012. DOI: 10.3779/j.issn.1009-3419.2012.08.11

51. Davidson MR, Larsen JE, Yang IA, Hayward NK, Clarke BE, Duhig EE, Passmore LH, Bowman RV, Fong KM: MicroRNA-218 is deleted and downregulated in lung squamous cell carcinoma. *PLoS One*, 5 (9): e12560, 2010. DOI: 10.1371/journal.pone.0012560

52. Wu DW, Cheng YW, Wang J, Chen CY, Lee H: Paxillin predicts survival and relapse in non-small cell lung cancer by microRNA-218 targeting. *Cancer Res*, 70 (24): 10392-10401, 2010. DOI: 10.1158/0008-5472.CAN-10-2341

53. Chen P, Zhao YL, Li YJ: MiR-218 inhibits migration and invasion of lung cancer cell by regulating Robo1 expression. *Chin J Lung Cancer*, 20 (7): 452-458, 2017. DOI: 10.3779/j.issn.1009-3419.2017.07.03

54. Gong XW, Zheng LM, Sheng DQ, Zhang LH: Research progress of miR-21 in non-small cell lung cancer. *Chin Bull Life Sci*, 30 (7): 765-770, 2018. DOI: 10.13376/j.cbls/2018091

55. Zhang XB, Peng F: Expression of microRNA-21 in peripheral blood and cancer tissues of patients with non-small cell lung cancer and its mechanism of involvement in tumor inhibition by regulating PTEN protein. *Chin J Gerontol*, 37 (22): 5571-5573, 2017.

56. Wang Y, Li JY, Tong LP, Zhang JW, Zhai AX, Xu K, Wei L, Chu M: The prognostic value of miR-21 and miR-155 in non-small-cell lung cancer: A meta-analysis. *Jpn J Clin Oncol*, 43 (8): 813-820, 2013. DOI: 10.1093/jjco/hyt084

57. Si ML, Zhu S, Wu H, Lu Z, Wu F, Mo YY: miR-21-mediated tumor growth. *Oncogene*, 26, 2799-2803, 2007. DOI: 10.1038/sj.onc.1210083

58. Wang XC, Wang W, Zhang ZB, Zhao J, Tan XG, Luo JC: Overexpression of miRNA-21 promotes radiation-resistance of non-small cell lung cancer. *Radiat Oncol*, 8:146, 2013. DOI: 10.1186/1748-717X-8-146